QUASI-STATIC AND DYNAMIC COMPACTION OF POROUS MATERIALS

Yehuda Partom

RAFAEL, Haifa, ISRAEL

‘From Static to dynamic’, London, 22-23 February 2010.

Outline

Herrmann's EOS

Instantaneous Pore Collapse

Gradual Pore Collapse

- Hugoniot curve
- Hydro-code Implementation

Quasi-static Spherical Shell model

- Semi-analytical Solution
- Numerical Solution

Dynamic Spherical Shell Model

- Semi-analytical Solution
- Hydro-code Implementation

Dynamic Overstress Model

Herrmann's EOS

EOS for porous solids goes back to Herrmann [1].

He assumed that:

$$E(P, V) = E_m(P_m, V_m) \;\; ; \;\; \text{m for matrix}$$

$$P_m = \alpha P \quad ; \quad \alpha = \frac{V}{V_m} = \frac{\rho_m}{\rho}$$

$$E = E_m\left(\alpha P, \frac{V}{\alpha}\right)$$

Herrmann's assumption $P_m = \alpha P$ needs to be checked on the mesoscale, but we adopt it anyway.

To complete the EOS one needs a relation $\alpha(P)$. In his well known Pα model Herrmann assumes a $P(\alpha)$ polynomial, to be calibrated from tests. Part of what follows is about choosing or calculating an $\alpha(P)$ (or $\varphi(P)$, $\varphi = 1 - 1/\alpha$) relation.

Instantaneous Pore Collapse

This is a popular model and has many names.

It assumes that for P=0+: φ(=porosity)=0, or α=1, and: V_m=V, P_m=P, E_m=E.

For the matrix we often use a Mie-Gruneisen EOS referred to the principal Hugoniot curve. We have:

$$E = E_H(V) + \frac{V_{m0}}{\Gamma_{m0}}\left(P - P_H(V)\right)$$

$$E_H(V) = \tfrac{1}{2} P_H(V)\left(V_{m0} - V\right)$$

$$\frac{V}{\Gamma} = \frac{V_{m0}}{\Gamma_{m0}}$$

The Hugoniot curve of the porous material, obtained by eliminating E from the EOS and the energy equation: $E = \tfrac{1}{2} P\left(V_0 - V\right)$ is:

$$P = P_H(V)\frac{V_{m0}/\Gamma_{m0} - \tfrac{1}{2}\left(V_{m0} - V\right)}{V_{m0}/\Gamma_{m0} - \tfrac{1}{2}\left(V_0 - V\right)}$$

It is well known that for high porosities (>40%) the Hugoniot curves extend to the right of $V=V_{m0}$. Using the above equation in this case means, that we rely on extrapolating the Hugoniot curve into the tension regime.

Instead we use the axis P=0 as the reference curve. We get:

$$P_{ref} = 0 \quad ; \quad E_{ref} = \frac{C_p}{\beta} \ell n \frac{v}{V_{m0}}$$

$$E = E_{ref} + \frac{V_{m0}}{\Gamma_{m0}} P$$

$$P = \frac{\frac{C_p}{\beta} \ell n \frac{V}{V_{m0}}}{\frac{1}{2}\left(V_0 - V\right) - \frac{V_{m0}}{\Gamma_{m0}}}$$

Implementing this instantaneous pore collapse model into a hydro-code we find that by using the axis as the reference curve for $V>V_{m0}$ we get much less noise at the shock level.

Gradual Pore Collapse

Hugoniot curve

Many times details of the pore collapse process are of interest. We then use gradual pore collapse models.

When $\varphi(P)$ is known or assumed, we can use Herrmann's EOS directly.

Two examples:

1. Exponential pore collapse curve $P_{PC}(\varphi)$:

$$P = P_c \exp\left(-\frac{\varphi}{\varphi_{ref}}\right)$$

where P_c is the pore closure pressure.

$$\varphi = \varphi_{ref} \ln \frac{P_c}{P}$$

2. Spherical shell plastic pore collapse (see later):

$$P = \tfrac{2}{3} Y_m \ln\left(\frac{1}{\varphi + \delta}\right)$$

$$\varphi + \delta = \exp\left(-\tfrac{3}{2}\frac{P}{Y_m}\right) \quad ; \quad \delta = \text{small number like } 10^{-4}$$

We introduce δ to avoid P going to infinity when φ goes to zero.

The pore collapse curve is also the elastic limit in compression.

For an initial porosity φ_0, pressure increases elastically without change of porosity until the pore collapse curve is reached.

The elastic limit is given by:

$$P_{EL} = P_{PC}\left(\varphi_0\right)$$

$$P_{EL} = \left(K + \tfrac{4}{3}G\right)\left(1 - \frac{V_{EL}}{V_0}\right)$$

where the degraded modulii are given by Eshelby's solution as:

$$\frac{1}{K} = \frac{1}{1-\varphi}\frac{1}{K_m} + \frac{3}{4}\frac{\varphi}{1-\varphi}\frac{1}{G_m}$$

$$G = \frac{1-\varphi}{1+\tfrac{1}{2}\varphi}G_m$$

The Hugoniot curve centered at the elastic limit is then given by:

$$E = E_{EL} + \tfrac{1}{2}\left(P + P_{EL}\right)\left(V_{EL} - V\right)$$

$$E = E_{Hm} + \frac{V_{m0}}{\Gamma_{m0}}\left(\frac{P}{1-\varphi} - P_{Hm}\right)$$

In Figs. 1 and 2 we compare two calculated Hugoniot curves for porous SS with 20% initial porosity. 1. Gradual pore collapse. 2. Instantaneous pore collapse.

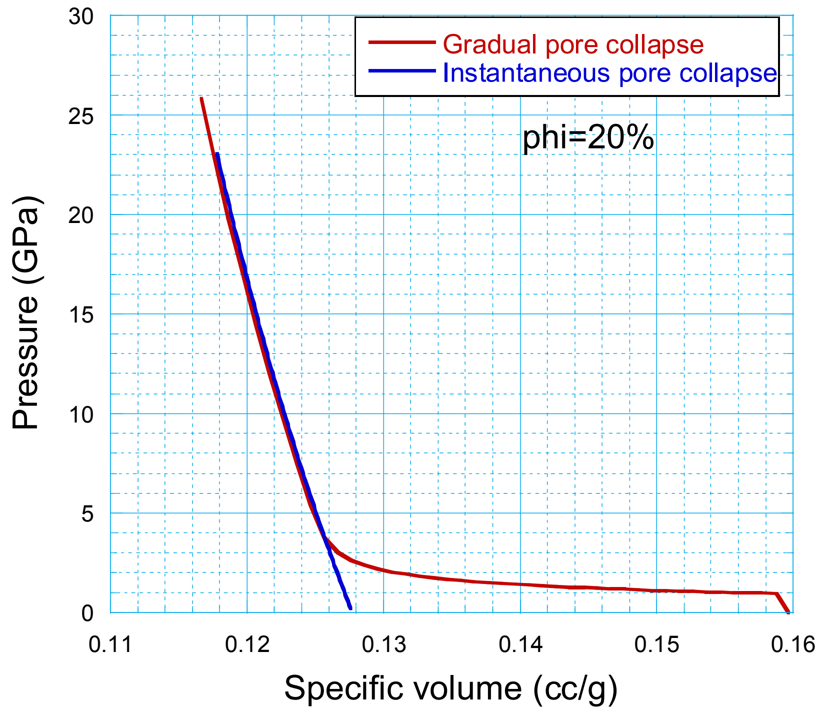

Fig. 1

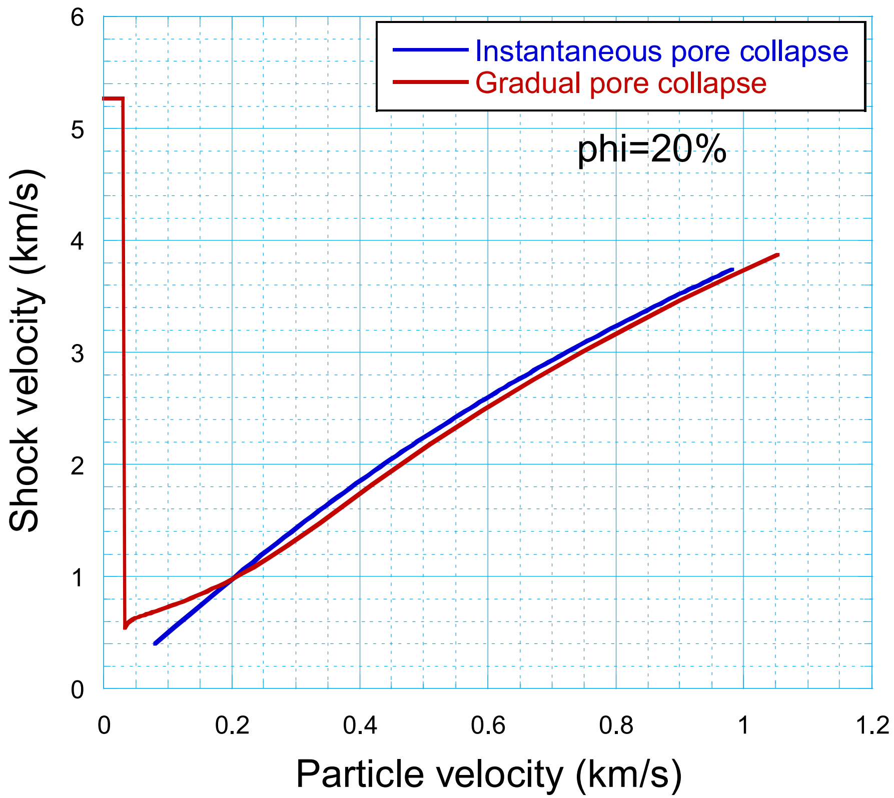

Fig. 2

Hydro-code implementation

The EOS is generally given by:

$$E = E(P, V, \varphi)$$

$$dE = \frac{\partial E}{\partial P} dP + \frac{\partial E}{\partial V} dV + \frac{\partial E}{\partial \varphi} d\varphi$$

Using: $\varphi = \varphi(P)$

$$d\varphi = \frac{d\varphi}{dP} dP$$

We get: $$dE = \left(\frac{\partial E}{\partial P} + \frac{\partial E}{\partial \varphi} \frac{d\varphi}{dP} \right) dP + \frac{\partial E}{\partial V} dV$$

and together with: $dE = -(P + q) dV$ We get finally:

$$\frac{dP}{dV} = \frac{P + q + \dfrac{\partial E}{\partial V}}{\dfrac{\partial E}{\partial P} + \dfrac{\partial E}{\partial \varphi} \dfrac{d\varphi}{dP}}$$

and the partial derivatives above are given by:

$$\frac{\partial E}{\partial P} = \frac{\partial E}{\partial P_m} \frac{\partial P_m}{\partial P} = \frac{1}{1-\varphi} \frac{\partial E}{\partial P_m}$$

$$\frac{\partial E}{\partial V} = \frac{\partial E}{\partial V_m} \frac{\partial V_m}{\partial V} = (1-\varphi) \frac{\partial E}{\partial V_m}$$

$$\frac{\partial E}{\partial \varphi} = \frac{\partial E}{\partial P_m} \frac{\partial P_m}{\partial \varphi} + \frac{\partial E}{\partial V_m} \frac{\partial V_m}{\partial \varphi} = \frac{P}{(1-\varphi)^2} \frac{\partial E}{\partial P_m} - V \frac{\partial E}{\partial V_m}$$

We get two first order ODEs to integrate for each computational cell at the EOS/energy stage of each time step: dP/dV=   and dφ/dV= . V_i and V_f are given, and we assume that V varies linearly between them.

Fig. 3 is a history plot of a planar impact calculation where a 20 GPa shock enters a 20% porous SS sample. We show P(V) and compare it to the Hugoniot curve in Fig. 1.

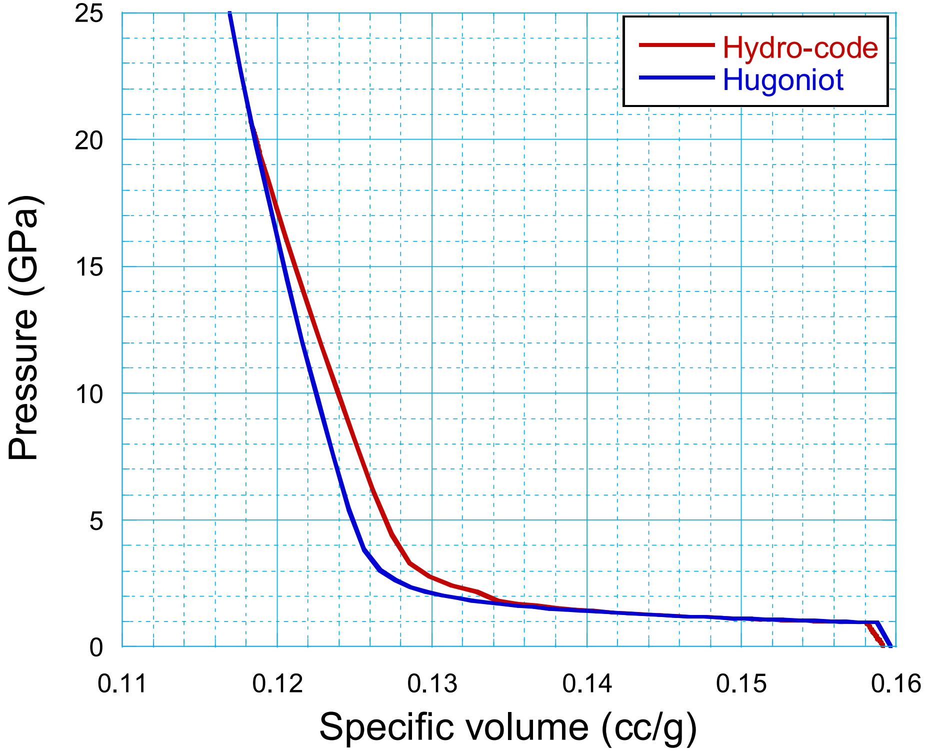

Fig. 3

Quasi-static spherical shell model

Semi analytical solution

Another way of assessing pore collapse mechanics is through a model on the mesoscale. Carroll & Holt (C&H) [2] used a spherical shell model. It is named after them, although they were not the first to use it. They developed a quasi-static solution and a dynamic solution, but assumed an incompressible matrix.

We develop similar solutions, and we take density changes into account. Our equations don't look identical to those of C&H.

There are 3 stages as function of the boundary pressure P_b: 1. Elastic, 2. Elastic-plastic and 3. fully plastic.

The elastic stage ends when:

$$a = a_0\left[1 + \tfrac{2}{3}Y\left(\tfrac{1}{3K} + \tfrac{1}{4G}\right)\right]^{-1}$$

a=inner boundary

$$b = b_0\left[1 + \tfrac{2}{3}Y\left(\tfrac{1}{3K} + \tfrac{\varphi}{4G}\right)\right]^{-1}$$

b=outer boundary

$$\varphi = \frac{a^3}{b^3} \quad ; \quad P_b = \tfrac{2}{3}Y(1-\varphi)$$

At the elastic-plastic stage there are 4 unknowns: a, b, P_b and the elastic-plastic boundary radius c. If one of them is specified, the others can be determined. It is easiest to specify a. Doing that we get 3 equations with 3 unknowns. The equations express: 1. Equation for b from the elastic field solution. 2. Continuity of σ_r across the elastic-plastic boundary. 3. mass conservation. Density changes are included in the third equation by assuming:

$$\rho = \rho_0\left(1+\frac{P}{K}\right)$$

The 3 equations are:

$$b = b_0 - \frac{b}{3K}\left(P_b + \tfrac{2}{3}Y\frac{c^3}{b^3}\right) - \frac{Y}{6G}\frac{c^3}{b^2}$$

$$2Y\ell n\frac{c}{a} = P_b - \tfrac{2}{3}Y\left(1-\frac{c^3}{b^3}\right)$$

$$c^3 - a^3 + 2\frac{Y}{K}c^3\ell n\frac{c}{a} + \left(1+\frac{P_b}{K}+\tfrac{2}{3}\frac{Y}{K}\frac{c^3}{b^3}\right)\left(b^3 - c^3\right) = b_0^3 - a_0^3$$

To solve these equations we differentiate them with respect to a and integrate numerically the system of 3 first order ODEs.

If and when c reaches the outer boundary (c=b) we enter the fully plastic stage. We have 2 equations: $P_b=\sigma_r(b)$ and mass conservation:

$$P_b = 2Y\ell n\frac{b}{a}$$

$$b^3 - a^3 + 2\frac{Y}{K}b^3\ell n\frac{b}{a} = b_0^3 - a_0^3$$

These can be solved directly by first eliminating $2Y\ell n\frac{b}{a}$.

In Figs. 4 we show results of an example for porous SS with 5 initial porosities φ_0=20%, 10%, 1%, 0.1%, 0.01%. In all the calculations b_0=1mm and a_0 has values according to these porosities.

In Figs. 5 we show the $P_b(\varphi)$ curves during the pore collapse.

In Fig. 6 we show the $P_b(\varphi)$ curve when a becomes less then 0.0001 mm.

We see from the figures that:

• When φ_0>1%, the elastic-plastic boundary reaches the outer boundary, and most of the collapse is fully plastic.

• When φ_0<1%, the elastic plastic boundary approaches the outer boundary, but then turns around and goes back.

• When φ_0 is very small, the elastic-plastic boundary stays close to the inner boundary, and the pore closure pressure is finite and tends to 2/3Y, as seen from Fig. 6.

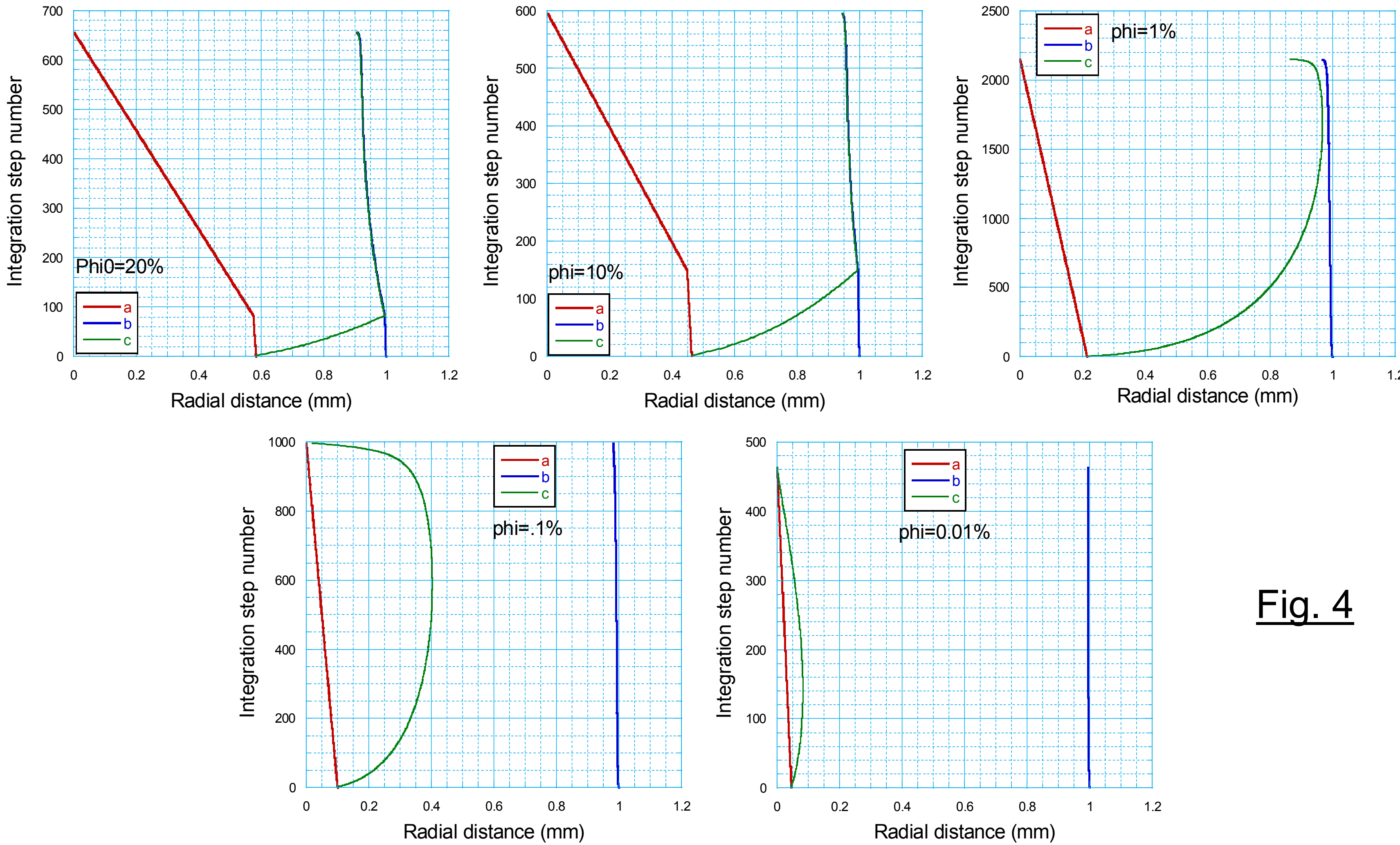

Fig. 4

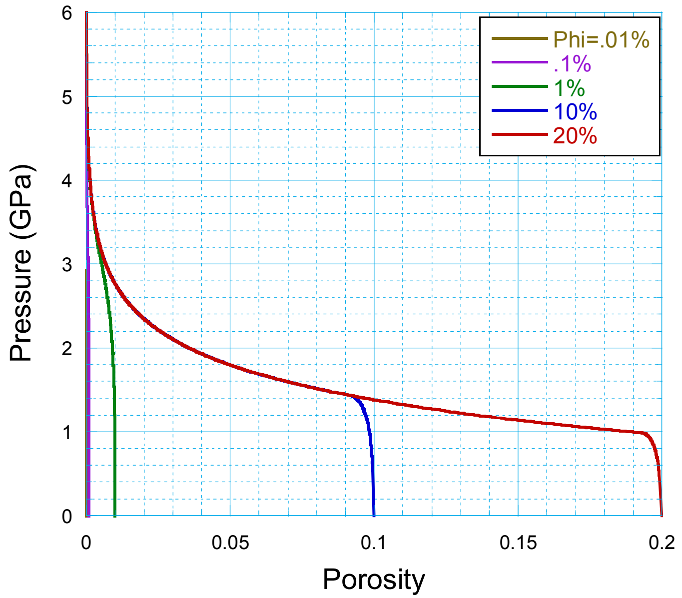

Phi=.01%
.1%
1%
10%
20%
Pressure (GPa)
Porosity

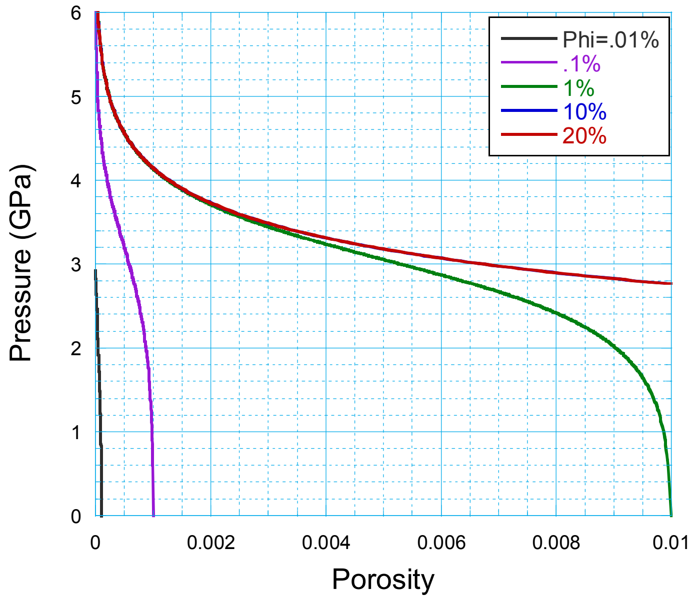

Phi=.01%
.1%
1%
10%
20%
Pressure (GPa)
Porosity

Fig. 5

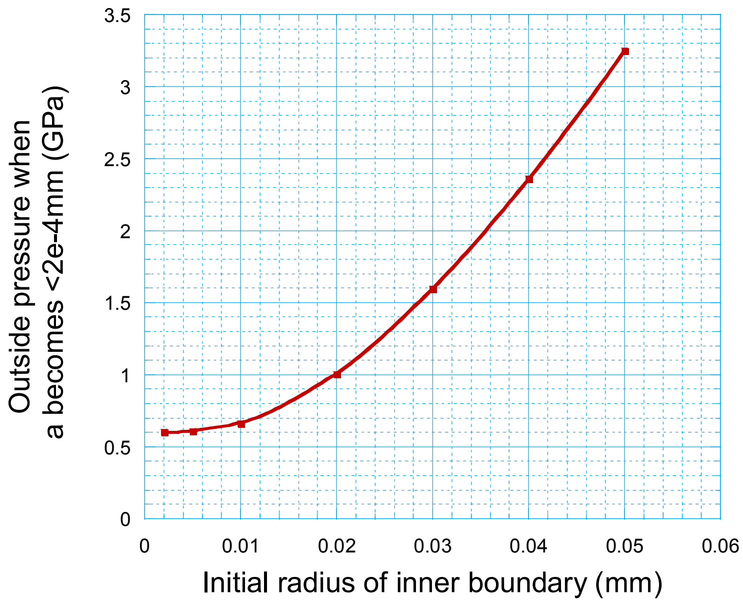

Outside pressure when
a becomes <2e-4mm (GPa)
Initial radius of inner boundary (mm)

Fig. 6

Numerical solution

It provides a check to the semi-analytical solution.

It makes it possible to include more general elasto-plastic, visco-plastic and failure behavior.

The solution details are:

• Divide the shell thickness into Lagrange cells Δr.

• For each integration step specify the displacement of the inner boundary Δa.

• Unknowns for each integration step are the cell boundary displacements u_i.

• Unknowns are determined from equilibrium equations for the staggered cells, which are:

$$F = \frac{\partial \sigma_r}{\partial r} + \frac{2}{r}\left(\sigma_r - \sigma_s\right) = 0$$

• Using finite differences we get the system of equations: $F_i\left(u_j, P_b\right) = 0$

• Solve the system iteratively with the Newton-Raphson scheme. For any approximation:

$$F_i\left(u_j, P_b\right) = R_i$$

• Corrections to the unknowns are obtained by solving the linear system:

$$\frac{\partial F_i}{\partial u_j}\Delta u_i + \frac{\partial F_i}{\partial P_b}\Delta P_b = -R_i$$

•The partial derivatives are determined by numerical differentiation. The system is tri-diagonal, but because u_0 is given, it can be solved recursively in one sweep.

In Fig. 7 we compare with the semi-analytical solution for an initial porosity of 20%. In the numerical solution we let the material fail (lose its strength) linearly between effective plastic strain of 0.3 and 1.0.

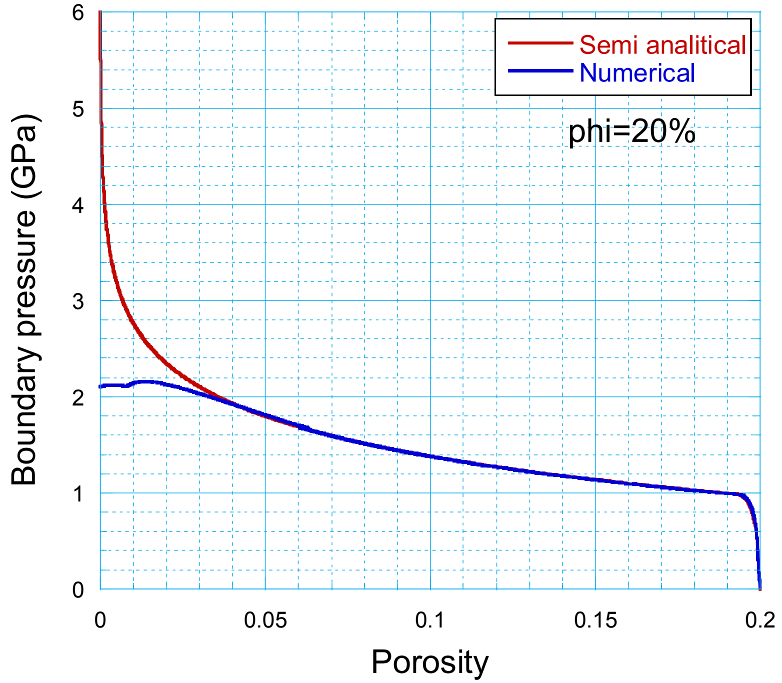

Fig. 7

Dynamic spherical shell model

Semi analytical solution

Without density changes

Mass conservation equation is:

$$\dot{\rho} = \rho\left(\frac{\partial v}{\partial r} + \frac{2}{r}v\right) = 0$$

where v is the radial velocity.

$$\dot{\rho} = 0 \quad \therefore \left(\frac{\partial v}{\partial r} + \frac{2}{r}v\right)$$

Integrating with respect to r we get:

$$\frac{1}{r^2}\frac{\partial}{\partial r}\left(vr^2\right) = 0 \quad ; \quad \frac{\partial}{\partial r}\left(vr^2\right) = 0$$

$$\int_a^r d\left(vr^2\right) = 0 \quad ; \quad vr^2 = \dot{a}\,a^2$$

$$v^2 = \frac{a^4\dot{a}^2}{r^4}$$

The momentum equation is:

$$\rho_0\dot{v} + \frac{\partial \sigma_r}{\partial r} + \frac{2}{r}\left(\sigma_r - \sigma_s\right) = 0$$

For $\dot{V}$ we get:

$$\dot{v} = \frac{\partial v}{\partial t} + v\frac{\partial v}{\partial r} = \frac{1}{r^2}\left(a^2\ddot{a} + 2a\dot{a}^2\right) + \tfrac{1}{2}\frac{\partial}{\partial r}\frac{a^4\dot{a}^2}{r^4}$$

Also, we approximate the stress deviator by its average as:

$$\sigma_r - \sigma_s \cong \overline{\sigma}_r - \overline{\sigma}_s = 2G\left(\overline{\varepsilon}_r - \overline{\varepsilon}_s\right) = 2G\left(\frac{b_0 - a_0}{b - a} - \frac{b_0 + a_0}{b + a}\right)$$

and check that: $\left|\overline{\sigma}_r - \overline{\sigma}_s\right| \le Y$

Finally, substituting into the momentum equation and integrating from a to b we get:

$$\left(a^2\ddot{a} + 2a\dot{a}^2\right)\left(\frac{1}{b} - \frac{1}{a}\right) = \frac{P_b}{\rho} + \tfrac{1}{2}a^4\dot{a}^2\left(\frac{1}{b^4} - \frac{1}{a^4}\right) + \frac{2}{\rho}\ell n\frac{b}{a}\left(\overline{\sigma}_r - \overline{\sigma}_s\right)$$

$$\text{or schematically: } \ddot{a} = F\left(a_0, b_0, a, b, \dot{a}, P_b\right)$$

If P_b is given we get from this two simultaneous first order ODEs:

$$\dot{a} = z \quad ; \quad \dot{z} = F(a_0, b_0, a, b, z, P_b)$$

$$b^3 = a^3 + b_0^3 - a_0^3$$

which can be integrated numerically.

In Fig. 8 we show an example of results using these equations. Again, it is a SS shell with 20% porosity and P_b=20GPa.

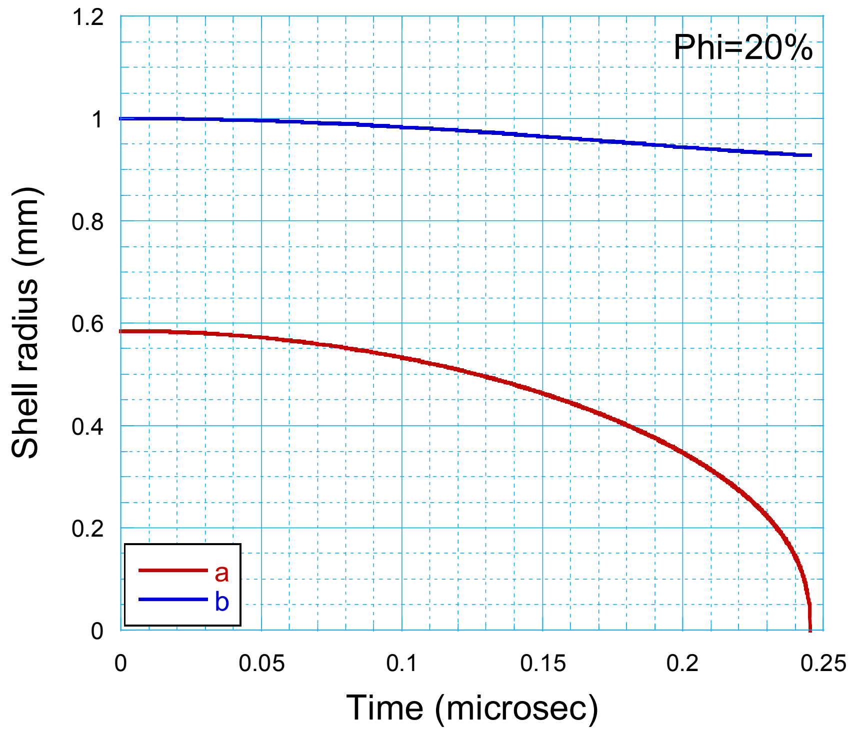

Fig. 8

We see from Fig. 8 that towards closure, the inner boundary velocity becomes extremely fast, and will probably get unstable.

We computed closure time as function of P_b. We show the results in Fig. 9.

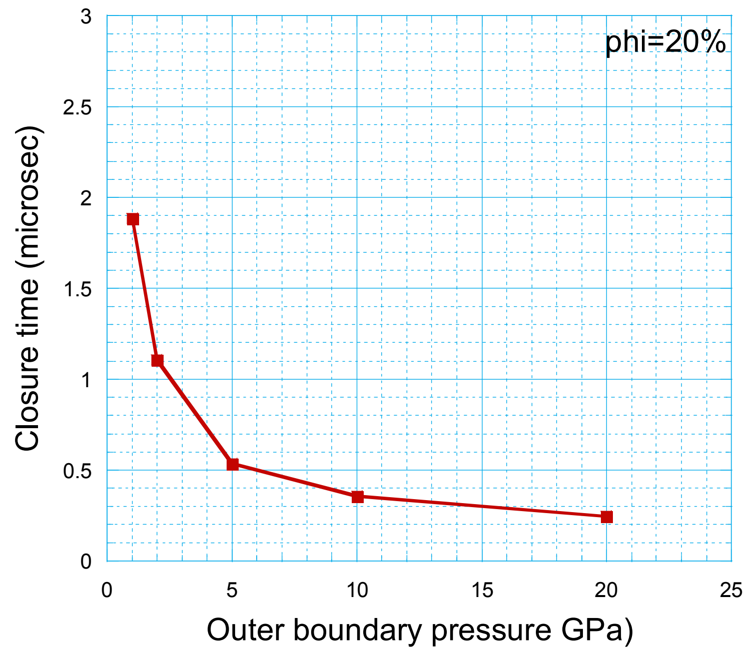

Fig. 9

We see from Fig. 9 that for P_b<1GPa the cavity does not close completely. This is different from the quasi-static solution. Also, we don't get an elastic-plastic stage, as we consider only averages of the shear stress components.

Including density changes

Using a similar approach, we're able to consider average density changes. The mass conservation equation is then:

$$\dot{\bar{\rho}}+\bar{\rho}\left(\frac{\partial \mathrm{v}}{\partial \mathrm{r}}+\frac{2}{\mathrm{r}}\mathrm{v}\right)=0 \quad ; \quad \left(\frac{\partial \mathrm{v}}{\partial \mathrm{r}}+\frac{2}{\mathrm{r}}\mathrm{v}\right)=-\frac{\dot{\bar{\rho}}}{\bar{\rho}}$$

As before we assume: $\bar{\rho}=\rho_0\left(1+\frac{\bar{P}}{K}\right) \quad ; \quad \bar{P}=P_b+\frac{2}{3}s$

$$\frac{\bar{\rho}}{\rho_0}=1+\frac{P_b+\frac{2}{3}s}{K} \quad ; \quad \frac{\dot{\bar{\rho}}}{\rho_0}=\frac{\dot{P}_b+\frac{2}{3}\dot{s}}{K}$$

$$\frac{\dot{\bar{\rho}}}{\bar{\rho}}=\frac{\dot{P}_b+\frac{2}{3}\dot{s}}{K+P_b+\frac{2}{3}s}$$

The momentum equation is: $\bar{\rho}\dot{\mathrm{v}}+\frac{\partial \sigma_r}{\partial r}+\frac{2}{r}\left(\bar{\sigma}_r-\bar{\sigma}_s\right)=0$

and the over whole mass conservation is: $b^3-a^3=\frac{\rho_0}{\bar{\rho}}\left(b_0^3-a_0^3\right)$

For a constant P_b the mass conservation equation is the same as before, and we may proceed as before (ignoring the small influence of the changing of s in the elastic region).

In Fig. 9 we show the porosity history for the same problem as before, and compare it to the result from the constant density run.

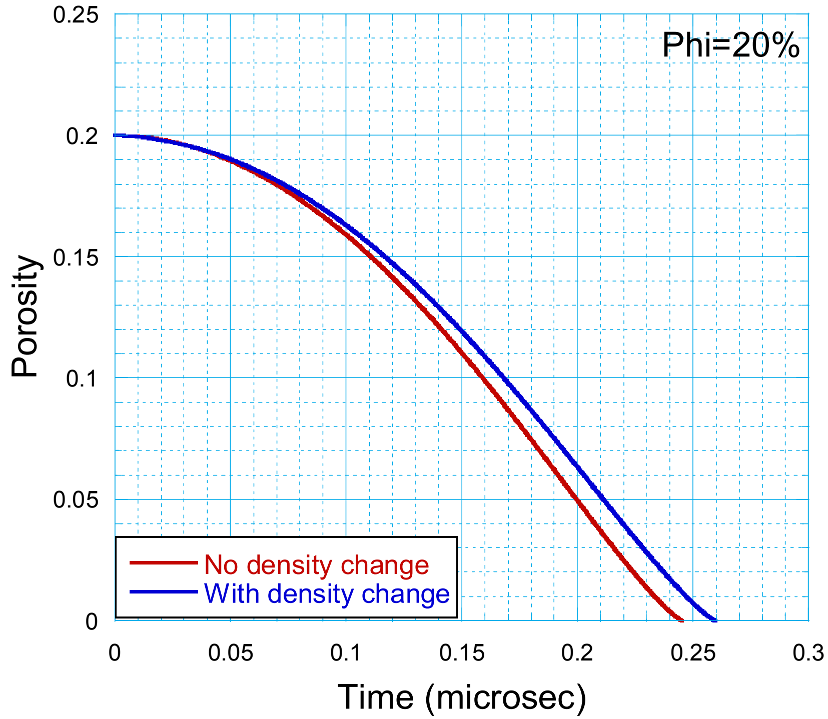

Fig. 9

We see from Fig. 9 that the influence of density change is small, and that it slows the compaction process.

If $P_b=P_b(t)$, the system of equations gets extremely complicated. We therefore chose not to work with these equations. Instead we approximate $P_b(t)$ by a staircase curve so that for each time step we have a constant P_b. The error introduced can be checked by changing the integration time step.

Implementing in a hydro-code

Similar to the implementation of the quasi-static model we have:

$$E = E\left(P, V, \varphi\right)$$

$$\dot{E} = \frac{\partial E}{\partial P}\dot{P} + \frac{\partial E}{\partial V}\dot{V} + \frac{\partial E}{\partial \varphi}\dot{\varphi}$$

$$\dot{E} = -\left(P + q\right)\dot{V}$$

$$\therefore\ \dot{P} = -\frac{P + q + \partial E/\partial V}{\partial E/\partial P}\dot{V} - \frac{\partial E/\partial \varphi}{\partial E/\partial P}\dot{\varphi}$$

Entering the material-energy stage, V_{new} for each computational cell at each time step is known, so that:

$$\dot{V} = \frac{V_{new} - V_{old}}{\Delta t}$$

Using this with the previous shell model equations, and identifying the matrix pressure and density with the average shell model pressure and density, we have:

$$\dot{a} = z \quad ; \quad \dot{z} = F(a_0, b_0, \rho, a, z, P_b)$$

$$b^3 = a^3 + \frac{\rho_0}{\overline{\rho}}\left(b_0^3 - a_0^3\right) \quad ; \quad \varphi = \frac{a^3}{b^3} \quad ; \quad \dot{\varphi} = 3\varphi(1-\varphi)\frac{z}{a}$$

$$P_m = \overline{P} \quad ; \quad \rho_m = \overline{\rho} \quad ; \quad P = (1-\varphi)P_m = (1-\varphi)\overline{P}$$

In Figs. 10 and 11 we compare results of a planar shock run with the dynamic shell model to that with the quasi-static shell model.

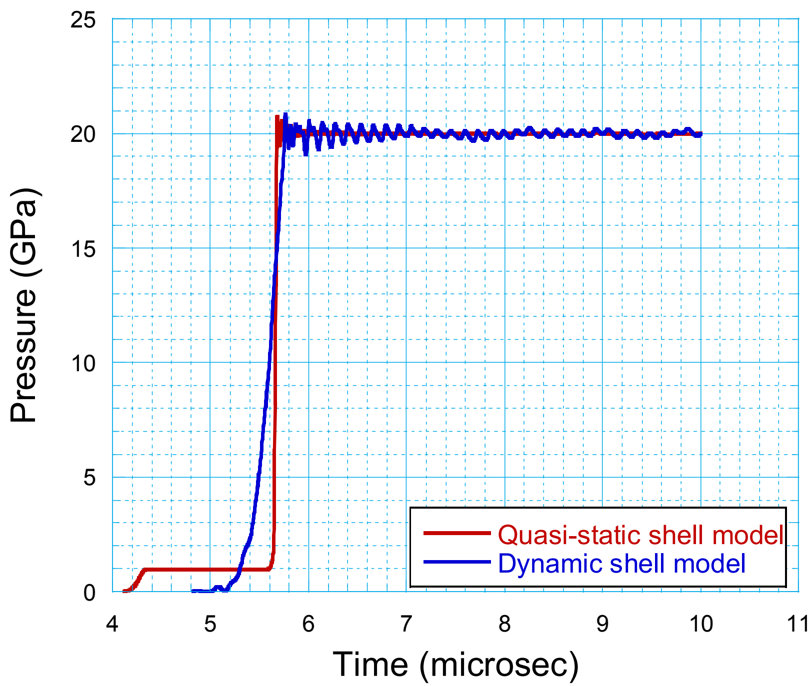

Fig. 10

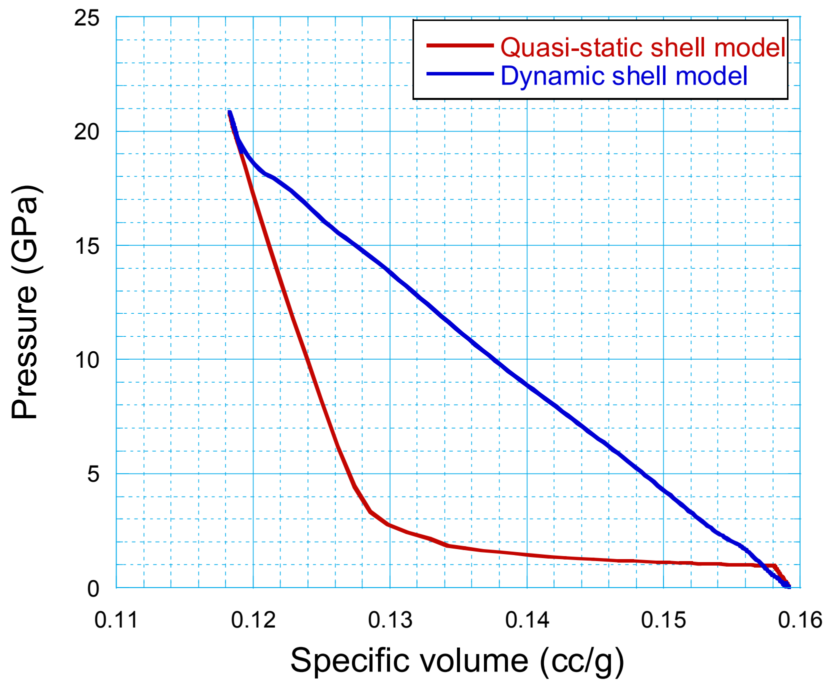

Fig. 11

We see that there is much difference between the quasi-static and the dynamic models:

• For the quasi-static model the pores close at a relatively low pressure, while for the dynamic model they close along the whole pressure range.

• For the dynamic model there is no elastic precursor.

• For the quasi-static model the shock is sharp, while for the dynamic model the shock is smeared, like for a visco-plastic material.

Dynamic overstress model

For dynamic problems that have an equilibrium or quasi-static solution, the system usually tends towards this solution at a certain rate.

Let the quasi-static solution be:

$$\varphi_{qs} = \varphi(P)$$

then, at any stage during the pore closure process we have by the overstress approach:

$$\dot{\varphi} = F\left(P - P_{qs}\left(\varphi\right)\right)$$

and the simplest form of this relation is:

$$\dot{\varphi} = -A\left(P - P_{qs}\left(\varphi\right)\right) \quad ; \quad \text{for } P > P_{qs}\left(\varphi\right)$$

where the coefficient A may be calibrated from tests. Combining this with the equation that we had before:

$$\dot{P} = -\frac{P + q + \partial E/\partial V}{\partial E/\partial P}\dot{V} - \frac{\partial E/\partial \varphi}{\partial E/\partial P}\dot{\varphi}$$

we get a system of two first order ODEs to integrate for each cell at each time step as before.

In Figs. 12 and 13 we show examples of such simulations with different values of A: 0.01 and 0.02 $(\mathrm{GPa}\ \mu\mathrm{s})^{-1}$.

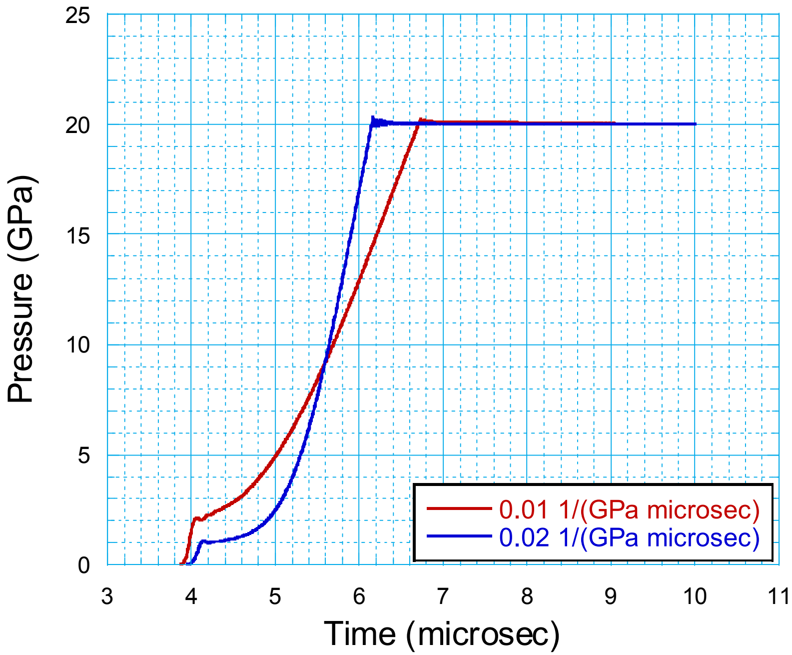

Fig. 12

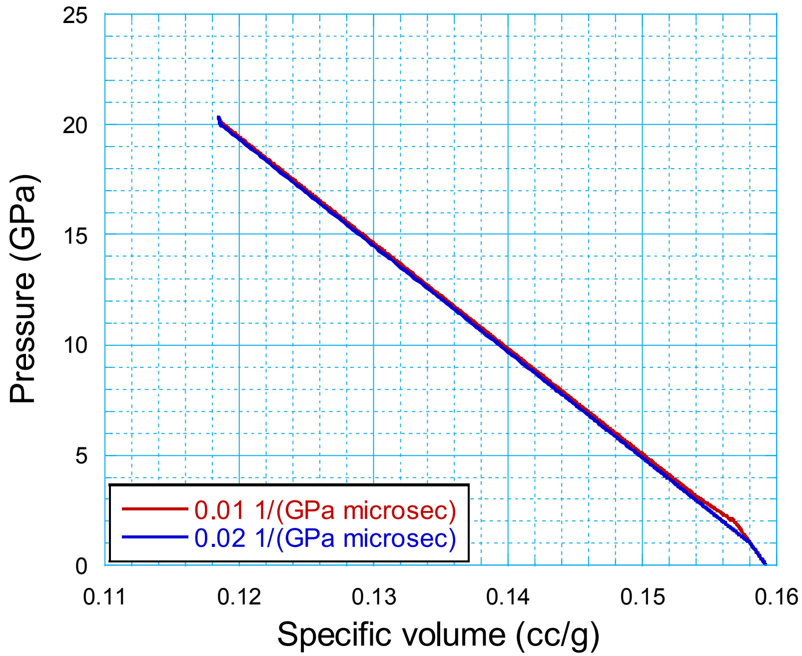

Fig. 13

We see from Figs. 12 and 13 that the rate coefficient determines the precursor level and the rise time. The P(V) curve is similar to that of the dynamic shell model, except for the precursor.

Summary

Modeling compaction of porous materials started with the pioneering works of Herrmann and Carroll & Holt in the sixties and seventies. Interest in the subject increased when explosive compaction became a viable technology. Never the less, the material models haven't changed much.

We present a survey of these models. They are based mainly on Herrmann's EOS and on Carroll & Holts spherical shell model. The examples we show are our own contribution, and the detailed equations are sometimes different from those in the original papers.

The subject is still open to more research because:

- A spherical shell does not represent all possible geometries.
- The models are mainly for ductile materials.
- Collapse under pressure + shear could give different results.
- The size distribution of pores could have an effect.